Mechanical behaviour of knit synthetic mesh used in hernia surgery

AGNIESZKA TOMASZEWSKA*

Gdańsk University of Technology, Faculty of Civil and Environmental Engineering.

Purpose: There is a discussion in literature concerning mechanical properties and modelling of surgical meshes. An important feature of elastic modulus dependency on load history is taken into account in this paper, as implants are subjected to variable loading during human activity. The example of DynaMesh®-IPOM surgical implant is studied. *Methods*: The analysis is based on failure tension tests and cyclic loading and unloading tests performed for the material samples. Stiffness changes of the material samples within successive load cycles are noted. The values the elastic modulus of the material tend to during successive cycles determine the material stiffness in the preconditioned state. The analysis is performed for two axes of the mesh, as the material reveals orthotropic properties. *Results*: For the initial displacements state of the material bilinear stiffness functions are determined for the two considered material axes. The functions for the preconditioned state are specified basing in the observed stiffness changes in subsequent loading cycles in experiments with different load (and strain) ranges. The identified elastic modulus values for different strain levels in the preconditioned state are then a basis for the nonlinear stiffness function formulation. *Conclusions*: The author concludes that two states of the considered mesh should be considered in calculations, initial and preconditioned ones. As the material stiffness in its preconditioned state is higher than in the initial one, omitting of the preconditioned state in calculation, e.g., considering fixation of the mesh, may lead to underestimation of necessary fixation strength.

Key words: *experiment; ventral hernia, surgical mesh, stiffness function, stiffening effect*

1. Introduction

Mechanical behaviour of a synthetic mesh used in laparoscopic ventral hernia (VH) repair is discussed in this paper. Ventral hernia is a serious and complex medical problem. Efficient treatment of VH (without recurrences) and reduction of chronic pain, which patients suffer from after an operation is still an open question [14]. Epidemiology shows quite a high risk of this sickness occurrence after a previous surgical intervention. For example, after major abdominal surgeries the risk rate is 12% and after laparoscopic operations it is 3.2% [2]. Besides, there are primary hernias caused by some primary defect of abdominal wall.

Mechanical point of view is important in searching for the best solution for VH treatment. Thus, mechanical behaviour of abdominal wall [7], [12], [13],

[18], of implants [9], [15], [17], and of fixations [1], [23], is experimentally studied. From analytical and numerical calculations the best solution for hernia operation can be specified, which means determination of an optimal implant to a given case and its fixation. All those works aim at improving ventral hernia treatment protocols.

Mathematical models for selected meshes implanted in human body are discussed in the literature. The models must be known in order to conduct any calculations in which implants are involved. For some implants used in hernia treatment one can find values of elastic moduli, e.g., in [17]. Other authors consider differences of the material behaviour in different directions and formulate anisotropic or orthotropic material models. For example, in [23], a linear elastic or bilinear elastic material model in two perpendicular directions distinguished for four kinds of implants are

---

* Corresponding author: Agnieszka Tomaszewska, Faculty of Civil and Environmental Engineering, Gdańsk University of Technology, ul. Narutowicza 11/12, 80-233 Gdańsk, Poland. Phone number: +48 58 348 64 03, e-mail: atomas@pg.gda.pl

presented. In paper [6], a finite element method model of a mesh implanted to the abdomen with a hyperelastic anisotropic material formulation for an implant is described. Those models are identified based on uni-axial tensile tests of the material samples.

Meshes implanted in the abdominal wall are subjected to cyclical loading during regular human activity (e.g., cough). In recent years, a stiffening effect occurring in cyclical loading of knit meshes has been reported [5], [9], [16], [24]. This effect causes the knit mesh to alter its state from an initial state to a preconditioned one with higher tension stiffness. In those papers general observations considering change of the stress-strain curve are reported.

In this paper, considerations concerning mechanical behaviour changes of a selected knit surgical implant due to load history are presented. The objective of the study is to determine stiffness functions of the mesh with reference to its states, initial or preconditioned. The stiffness functions are a basis for a quantitative assessment of the mesh stiffness change due to the state change and comments concerning the clinical implications.

2. Materials and methods

2.1. Material

DynaMesh®-IPOM surgical implant (FEG Textiltechnik mbH, Aachen, Germany) intended for VH operations is selected for this analysis. The mesh is a knitted structure, see Fig. 1, made of polypropylene (PP) and polyvinylidene fluoride (PVDF). Earlier uni-axial failure tests have shown that the material considered reveals different properties in various directions [23]. Its behaviour has already been modelled using orthotropic material model [20] or the dense-net material model [10], with directions of the net threads corresponding to orthogonality axes of the implant. The direction of the biggest material compliance is marked by green threads attached by the producer to one or two edges of the implant. This sets directions of the material orthogonality.

2.2. Samples and experiments

Five rectangular samples of the material have been cut form one piece of the implant in two perpendicular directions (orthogonality axes), as noted in Section 2.1. Let the axis of the biggest material compliance be marked by 1, and the perpendicular axis by 2. The di-

mensions of each sample are 30×120 mm. They are subjected to uni-axial stress state and the force vector is parallel to longer dimension of each sample. The two kinds of samples are presented in Fig. 1. Zwick Roell Z020 testing machine has been used in the experiments. The machine is dedicated to loads bigger than 100 N, however, it has been additionally calibrated in the force range 0–100 N. The device is equipped with a video extensometer whose resolution reaches 0.25 μm.
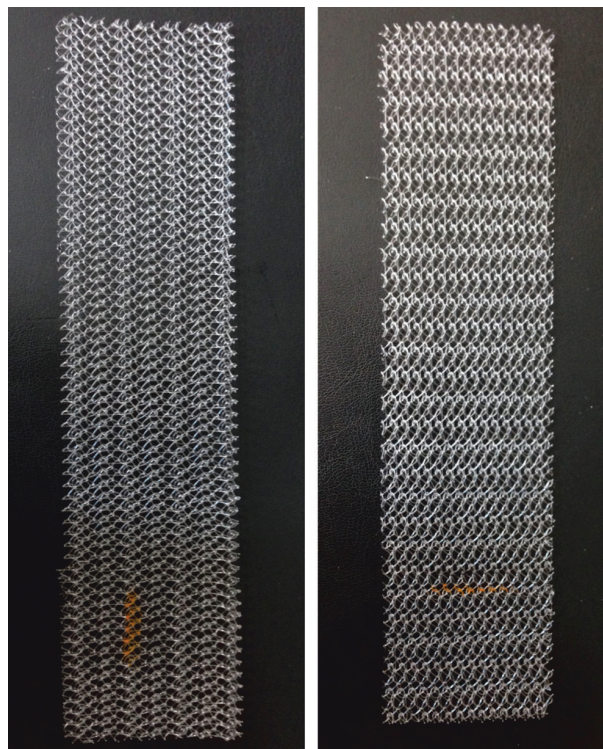

Fig. 1. Samples cut in the 1 direction of the mesh on the left hand side and in the 2 direction on the right hand side

The samples have been subjected to cyclical loading tests in uni-axial stress state at four different force ranges. Eleven load cycles have been programmed in each experiment. The force ranges relate to earlier studies concerning load capacity of connectors used in laparoscopic ventral hernia repair (see [23]). It appears that a single tack can carry maximal load of 10 N, whereas single trans-abdominal suture – 20 N for load applied in the direction 2 of the mesh and 35 N for direction 1 of the implant. In practise the connectors are typically arranged at intervals of 30 mm. In those experiments the width of samples equals 30 mm. Thus, it can be estimated that the load applied to the strips tested is the load acting on a single connector fixing the mesh to the abdominal wall (compare [22]). The force ranges considered are presented in Table 1. There are 10-second intervals at points of maxi-

Table 1. Description of experiment performed for a given sample

Orientation of the sample	Sample label	Applied force range in cyclic test [N]	Maximum force applied after cyclic load [N]	Strain rate applied [1/s]
"1"	1.0	failure tension test		0.001
	1.1(ex.1)	0.5÷2	10	
	1.2	0.5÷5	10	
	1.3	0.5÷10	20	
	1.1(ex.2)	0.5÷20	40	
	1.4	0.5÷10	25	0.03
"2"	2.0	failure tension test		0.001
	2.1 (ex.1)	0.5÷6	20	
	2.2	0.5÷10	50	
	2.1 (ex.2)	0.5÷15	50	
	2.3	0.5÷20	40	
	2.4	0.5÷10	40	0.03

mum/minimum force in each cycle. In order to compare stiffness of the material in its initial state and in the preconditioned one (after cyclical loading) one sample of each kind has been subjected to uni-axial failure tension test.

The experiments are performed with a strain rate of 0.001 1/s. Earlier tests have shown that stress-strain curves obtained in uni-axial tension experiments on DynaMesh®-IPOM are repetitive, even in the case of different strain rates applied to subsequent samples. For this reason each load case has been applied to one sample in this study. However, in order to check the influence of a strain rate on the results of a cyclical test, one of the load scenarios, with load values between 0.5 N and 10 N, has been repeated for the strain rate 0.03 1/s for both kinds of samples. The 0.001 1/s strain rate simulates very slow human movement, while 0.03 1/s – quite fast one. The values are discussed, e.g., in [21].

One specimen taken from each of the two groups has been loaded twice at an interval of two days. The ability of the material to restore itself to its initial state after some "rest time" is investigated. The samples are 1.1 and 2.1 so their labels have additional marks "(ex.1)" and "(ex.2)" to distinguish between the two successive experiments.

In each test initial distance between the machine jaws is 90 mm, while the measuring base of the extensometer is about 30 mm located in the middle of a sample. Initial load applied to samples amounts to 0.5 N. The experiments are force controlled.

2.3. Measured data processing

The testing machine measures force and elongation. In order to study mechanical behaviour of the material, those data are transformed into Biot(Engineering) Strains, defined as actual elongation divided by initial length of a specimen $\varepsilon = \dfrac{\Delta L}{L_0}$ [–] in uni-axial stress state, and Biot(Engineering) Stresses, calculated as actual force divided by initial width of a sample $T = \dfrac{P}{A_0} \left[\dfrac{\text{N}}{\text{mm}} \right]$. The kind of unit used here for stresses is typical in considerations of thin structures, like shells, membranes, etc. [8].

In order to reduce the noise in the measured force data, the resulting signals $T(\varepsilon)$ have been filtered using FFT (Fast Fourier Transform). In this procedure, the data are transformed from the ε domain to the $\dfrac{1}{\varepsilon}$ domain. The response of a structure one can find for lower values in this domain, while noise is visible for higher values of $\dfrac{1}{\varepsilon}$. In this new domain it is easy to remove unwanted part of a signal by using, for example, some digital filter. In this research MATLAB environment has been applied for this purpose and the function *ellip*. Parameters of the filter are selected individually for each signal in relation to its representation in the $\dfrac{1}{\varepsilon}$ domain. Such a procedure is typical in signal processing (see, e.g., [11]), it is fast and convenient.

2.4. Stiffness function identification

In order to determine the stiffness functions of the two states of the material two kinds of experiments have been conducted. The functions are de-

rived based on simple tension states for the initial state of the material when no load history is recorded for the mesh. Based on cyclical loading and unloading tests the stiffness functions are specified for the material in the preconditioned state recording the load history. The stiffness functions have been identified in the following manner. The nonlinear stress-strain relations measured in simple tensile tests (Fig. 2) are idealised by bilinear functions, so that different values of elastic modulus E_i are for lower strains range in the two directions of the mesh and different are for higher strains range. The obtained E_i values describe piecewise constant stiffness functions F_i of the material in its initial state.
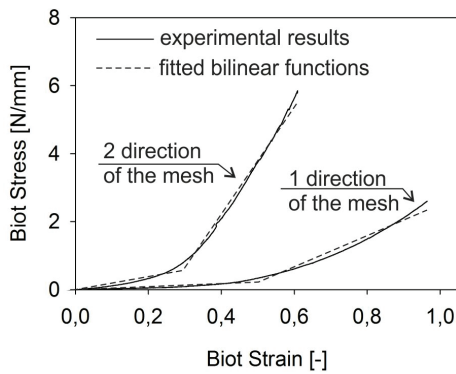
Fig. 2. Stress-strain relations obtained from failure tension tests and results of bilinear functions fitting

From the cyclical loading and unloading tests stiffness of the material being in the preconditioned state can be identified, however, starting from the second load cycle. In the first cycle, the material is always in the initial state, so that parts of the experiments are used to confirm results of the failure tests. A single cyclical test was conducted for a certain load range and for a certain strain range of the material (Fig. 3). Thus, the analysis conducted for a single cyclical test is valid for a strain range covered by stress-strain hysteresis loops in the test considered. In this approach, only the loading parts of the experiment are taken into account. The following steps of the analysis can be enumerated:

1. The elastic modulus E of the material is determined for each hysteresis loop separately as a tangent of the stress-strain relation for the upper, slightly curved part of the hysteresis considered (Fig. 4). The recorded E values are valid for the strains covered by the analysed hysteresis parts, as marked in Fig. 4.

2. The obtained E values are plotted against the population of load cycles. The plot detects variations in material stiffness within successive loading scenarios. This discrete plot is approximated by a relevant function and then extrapolated to 100 load cycles. A tendency is detected for the elastic modulus to stabilize at a certain level if a horizontal asymptote exists. The asymptote determines an elastic modulus value for the material in the preconditioned state E_p for the strain relevant to the analysed part of the stress-strain hysteresis loops in a given cyclical test.

3. All E_p values obtained from the analysis of all cyclical tests performed for the 1 axis of the material are presented in a common plot in the strains domain – four values of E_p are plotted against the corresponding strains since four different experiments, performed with the same strain ratio, are considered. A similar process is conducted for the 2 direction of the material.

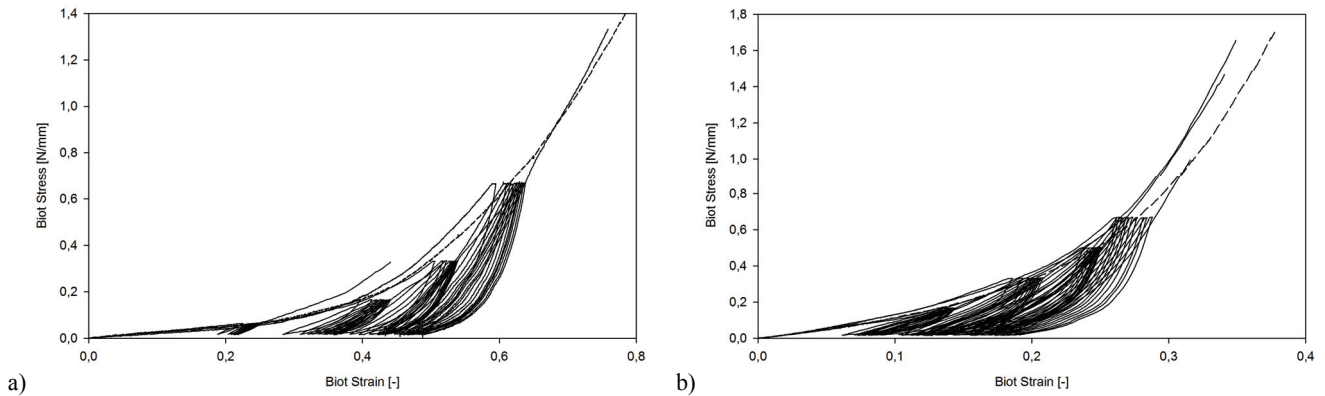4. The two discrete plots obtained in the previous step are finally approximated by nonlinear stiff-

Fig. 3. Stress-strain relations obtained from cyclic tests for samples (a) cut in 1 direction of the mesh (most compliant), (b) cut in 2 direction of the mesh (perpendicular to 1), for the strain rate 0.001 1/s; parts of the relations from the failure tension test are presented by dotted lines
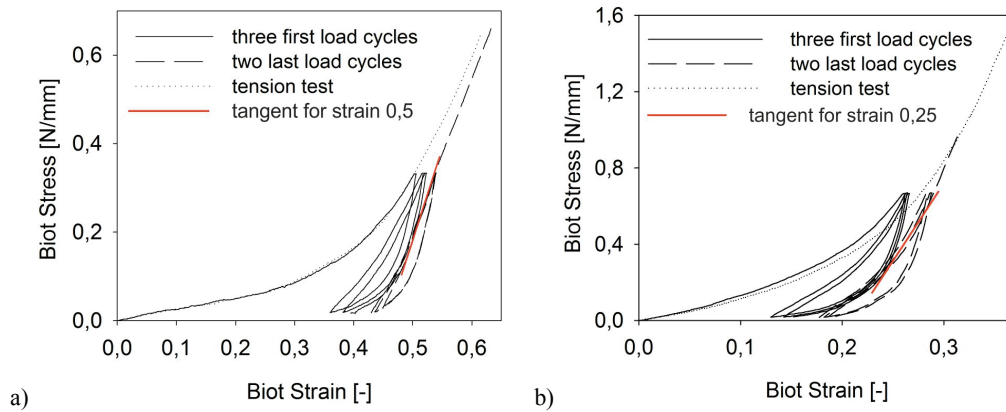
Fig. 4. Stress-strain relations obtained for the first three and two last load cycles
in two selected experiments and parts of the simple tension tests; samples: (a) 1.3, (b) 2.3

ness functions F_p for the material in its preconditioned state.

All functions used in the analysis are fitted to data sets in the optimization process using the Marquardt–Levenberg variant of the least squares method [3]. The Sigma Plot program (Systat Software Inc., San Jose, USA) has been used, and the assumed tolerance of the fitting functions is 1e-10.

3. Results

Stress-strain curves obtained in failure tension tests and the results of bilinear functions fitting are plotted in Fig. 2. The following elastic modulus values E_i are identified from the bilinear functions. For the mesh in the 1 direction the value is equal to 0.38 N/mm for strains smaller than 0.5 and 5.45 N/mm for bigger strains. For the mesh in the

2 direction it is equal to 1.8 N/mm for strains smaller than 0.3 and 17.8 N/mm for bigger strains. The samples ruptured for stress 2.60 N/mm (strain 0.964) and stress 5.78 N/mm (strain 0.607) in the 1 and 2 directions, respectively.

Stress-strain relations obtained for the cyclical load tests in the experiments with the strain rate 0.001 1/s are presented in Fig. 3. In Fig. 4, example tests for both kinds of samples are presented separately in order to note differences between first and last load cycles in the tests. Adequate parts of the failure tension tests are also plotted in those two figures for comparison. Figure 5 shows stress-strain relations obtained for the same load scenario for a given type of a sample but realised with different strain rates, 0.001 1/s for samples 1.3 and 2.2, and 0.03 1/s for samples 1.4 and 2.4.

In Fig. 6, diagrams of elastic modulus change in each subsequent load cycle in each test are presented. The values are plotted against the load cycle number. The numbers 2÷11 refer to subsequent loading cycles.
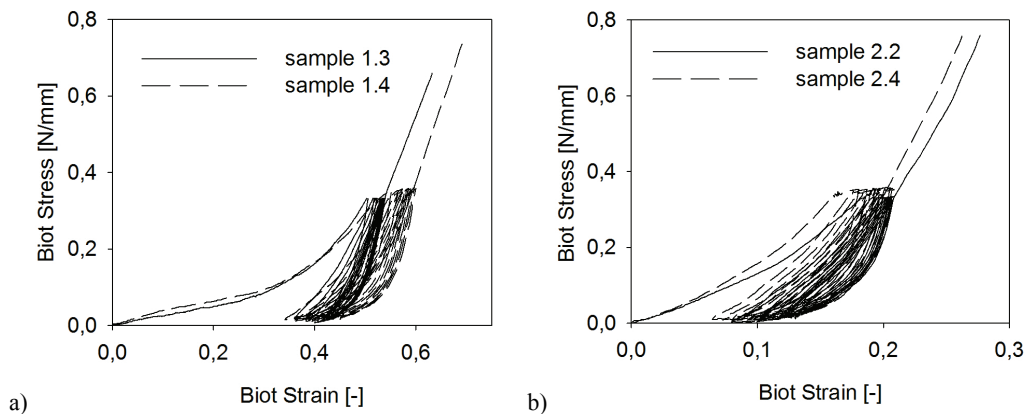

Fig. 5. Stress-strain relations obtained for the same load scenario but realised with different strain rates,
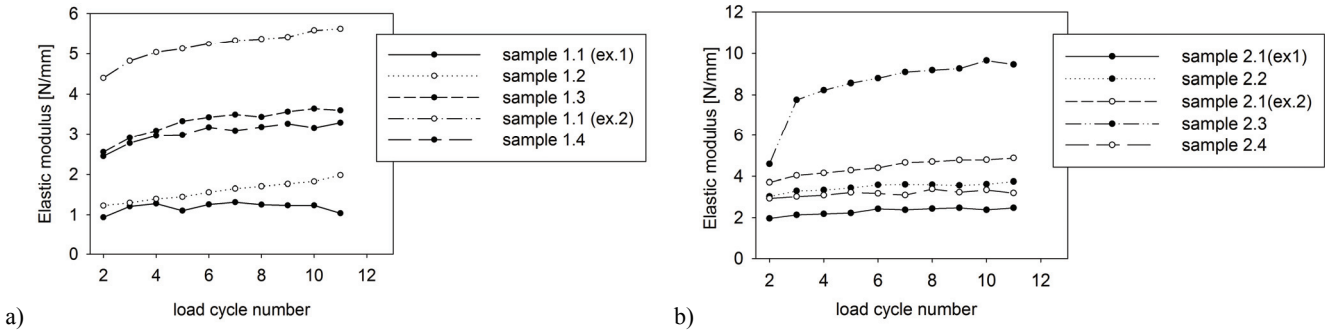0.001 1/s for samples 1.3 and 2.2, and 0.03 1/s for samples 1.4 and 2.4

Fig. 6. Values of elastic modulus identified for stress-strain curves corresponding to each loading path of subsequent cyclic tests,
(a) results for 1 direction of the mesh, (b) results for 2 direction

4. Discussion

Basic observation in this analysis is that stress-strain relation obtained for the initial material state, which are obtained in the failure tension tests and in the first load path in the cyclic tests are different from the relations obtained for subsequent load cycles. Similar observations are made for other polypropylene surgical meshes [9], [24]. Mechanical behaviour of DynaMesh®-IPOM in different load conditions is discussed here. In particular, the mesh tension stiffness variations under load history are analysed and stiffness functions are formulated for two states of the material.

Successive hysteresis loops in cyclic tests are rightward shifted (see Figs. 3, 4). Such a result indicates viscous creep or permanent elongation, depending on the level of load applied to a given sample. In the experiments performed, viscous creep is observed for samples 1.1 (ex. 1), 1.2, 1.3, 1.4, 2.1 (ex. 1), 2.2, 2.1(ex. 2), 2.4. Those specimens gained their initial lengths after the tests, however, within different time. For the samples subjected to the lowest load levels it took 3 hours and for the samples loaded by higher forces it took even three weeks. The other two samples stayed elongated three weeks after the tests, sample 1.1 (ex. 2) by 8% and sample 2.3 by 1%, so permanent deformations have occurred here in addition to viscous creep.

A comparison between hysteresis loops obtained in a single experiment indicates a stable behaviour of the material samples, as they do not differ much (in width or slope). As a few last loops are more similar to each other than a few first loops (see examples in Fig. 4), one can conclude that the material behaviour tends to stabilise within subsequent load loops. That stabilisation can be better observed in a phase portrait

of the experiment. Such example plot for the sample 1.1 (ex. 2) is presented in Fig. 7. For increasing or decreasing load value in the test fluctuations around horizontal lines in that plot are obtained. Almost vertical lines are obtained for the moments of load vector sense change. Some bigger perturbations of the strain – strain rate relation occur for each load path beginning (load increasing or load decreasing). That is visible in the upper left and lower right corners of the relation rectangle. Stabilisation of the material behaviour can be perfectly observed at the moments of the machine slowing down, as the distances between plots for the successive cycles are smaller and smaller. When the machine gathers speed the distances between strains – strains rate relations in subsequent load cycles become smaller, with one exception, which is between the eighth and ninth load cycle. Such one perturbation does not influence the general observation.
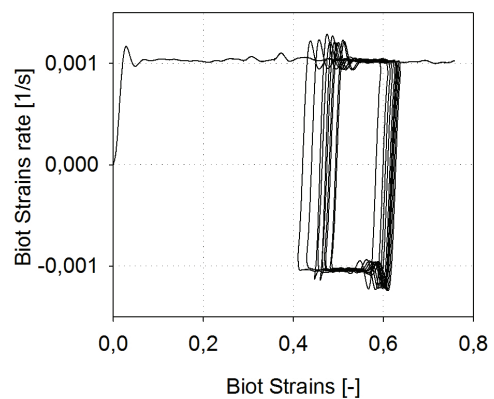

Fig. 7. Phase portrait of experiment on the sample 1.1 (ex. 2)

An effect of the material stabilisation within subsequent load cycles is visible also in Fig. 6, where values of elastic moduli for each loading path are presented. The shapes of the relations allow their

asymptotes to be found, which determine values of elastic moduli of the material in the preconditioned state, when it is constantly subjected to load, like it is often in reality, after the material implantation. The relations presented in Fig. 6 can be approximated with a high accuracy by a rational function given by the following equation

$$f(x) = \frac{1 + kx}{m + nx}, \qquad (1)$$

where k, m, n are the function parameters and x denotes the load cycle number. The regressions and extrapolations for 100 load cycles are presented in Fig. 8. Values of parameters identified for each relation are given in Table 2.

For each elastic modulus – load cycle number relation, presented in Fig. 8, a horizontal asymptote determines stiffness of the material in the preconditioned state, related to strain range covered by a given cyclic test. The elastic modulus values determined by

Table 2. Rational function (according to equation (1)) parameter values,
which fit the function to elastic moduli values identified for subsequent experiment

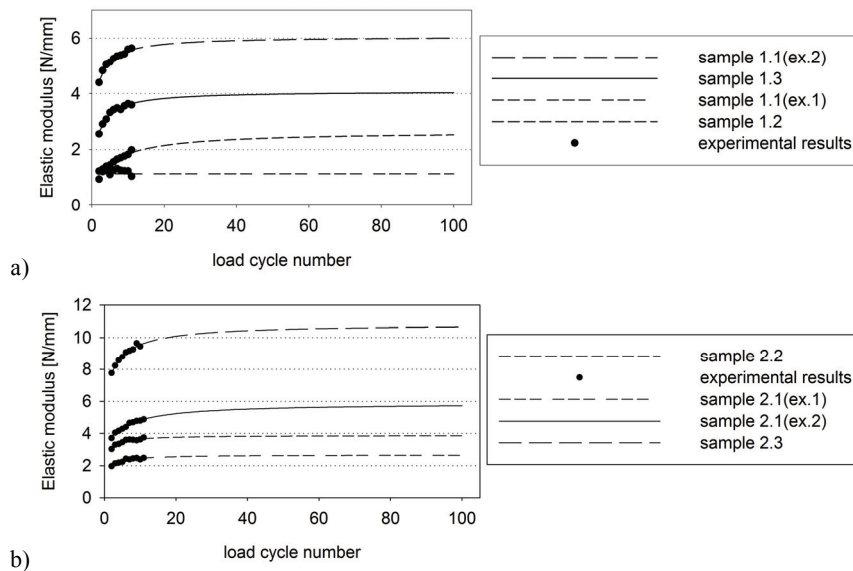| Parameter	Parameter value for the following sample:							
	1.1(ex.1)	1.2	1.3	1.1(ex.2)	2.1(ex.1)	2.2	2.1(ex.2)	2.3
k	−0.1429	0.6036	2.0647	1.4293	1.7914	5.2525	0.3499	0.4994
m	0.8813	1.5375	0.9534	0.4008	0.9957	1.0755	0.3369	0.1655
n	−0.1259	0.2283	0.5054	0.2359	0.6704	1.3548	0.0595	0.0462

a)

b)

Fig. 8. Elastic modulus values in relation to the number of load cycles,
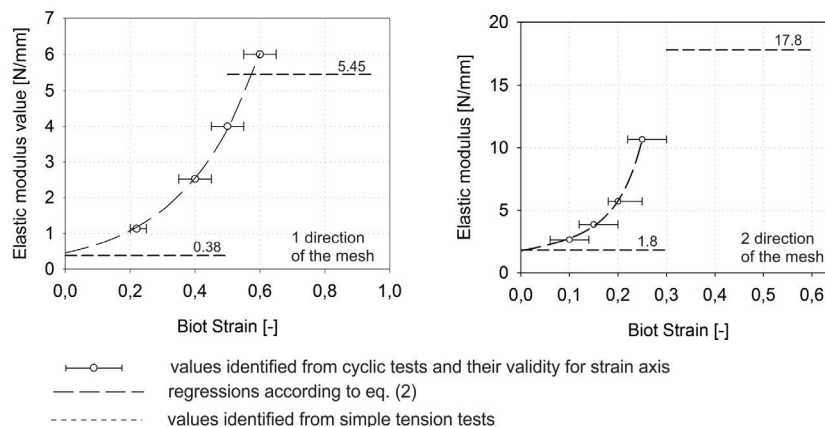(a) results for 1 direction of the mesh, (b) results for 2 direction

Fig. 9. Identified and predicted values of elastic moduli as a function of Biot Strains

the asymptotes are presented in Fig. 9. The corresponding strain ranges are specified based on the relations presented in Fig. 3, where strain ranges for each cyclical loading scenario can be noted. The obtained values are then the basic points for regression, which can describe elastic modulus as a function of strains. Exponential form of stiffness function has been selected for this purpose, in the following form

$$F_p(\varepsilon) = ae^{b\varepsilon} + ce^{d\varepsilon}, \qquad (2)$$

in which a, b, c, d denote parameters and ε stands for strains. Values of the parameters of the exponential function presented in Fig. 9 are given in Table 3.

Table 3. Exponential function (according to equation (2)) parameter values, used for elastic modulus values regression in the strains domain

Parameter	Parameter value for the "1" direction of the mesh	Parameter value for the "2" direction of the mesh
a	0.0265	0.0265
b	4.3138	21.8625
c	0.4269	1.7433
d	4.3138	3.6873

The regressions in Fig. 9 are extrapolated on lower strain values than covered by the cyclic tests and the function is plotted starting from zero strain point. On the other hand, extrapolation for higher strains than considered in experiments is not made as it would be an unnecessary speculation. The functions of elastic modulus cover strains in a range 0÷0.65 in the 1 direction and 0÷0.30 in the 2 direction. Taking into account possible, physiological strains on the internal surface of human abdominal wall [21], [13], that range is accurate.

Stress-strain relations obtained in two directions of the implant in the initial state are approximated by bilinear functions (see Section 3). Elastic modulus values describing the two functions are marked in Fig. 9. One can notice a considerable difference in the material stiffness when the material state changes from the initial to the preconditioned one. For example, for the 2 direction of the mesh the identified values of elastic modulus for strain 0.2 are 1.8 N/mm for initial state of the material and 5.5 N/mm for the preconditioned state, that is approximately a 3-fold increase. For the 1 direction of the mesh the elastic modulus values for strain 0.4 are 0.38 N/mm or initial state of the material and 2.6 N/mm for the preconditioned state, that is approximately a 7-fold increase. The mesh behaviour discussed certainly influences the persistence of her-

nia repair since the stiffness increase also increases the force acting on the mesh fasteners. Szymczak et al. [21] showed that doubling of the mesh stiffness raises this force by 10–35%. That change may result in overloading of a mesh fastener, possibly resulting in fixation damage and the recurrence of the sickness. Moreover, there is an increased risk of chronic pain when the mesh becomes stiffer [4]. The stiffness increase may be caused by friction between the yarns during stretching of the mesh and/or by strain hardening of the yarns themselves [9]. The findings presented here may be important for new mesh creation processes. The procedure described, for example, in [19] might be supplemented by experiments with cyclical loading.

The effects of the strain rate applied in cyclical tests are presented in Fig. 5. A 30-fold change in the strain rate has been made in the experiments compared (see Table 1) and the obtained stress-strain plots are quite similar. The similarity of the material behaviour in those two experiments is visible also in Fig. 6, where little changes of the elastic modulus values for samples 1.3 and 1.4, or for samples 2.2 and 2.4 can be observed. For the 30-fold strain rate increase, a 1.1-fold decrease of the moduli values is observed for the samples of both kinds. One can conclude that the strain rate applied in the experiment has a negligible influence on identification of the elastic modulus of DynaMesh®-IPOM.

The samples 1.1 and 2.1 have been tested twice at an interval of two days. This allowed the material behaviour to be observed after some "rest". Each time the samples revealed the same initial stiffness. This means that in practise the material can be in its initial state not only once. It can gain its initial stiffness after, e.g., dream of a patient, if permanent strains have not occurred.

The stiffness functions can be used in calculations concerning the mesh behaviour. Functional form of this relation has an additional advantage. It enables elastic modulus to be represented in relation to other strain measure than used in this research if a proper mathematical transformation for strains is made.

This analysis is made for loading only, unloading phases of cyclic tests are omitted. Thus, the material stiffness determined suits calculations with loading of an implant.

The present analysis concerns a mesh implanted to human abdominal wall. It is known that after a few weeks the implant is overgrown by a tissue and its stiffness changes. The author does not consider such a situation. Doctors claim that most relapses of the hernia occur in a period when the mesh has not been

surrounded by a collagen yet. Thus, that time is crucial for the success of the operation and that is why only a pure implant is considered in this analysis.

5. Conclusions

A discussion considering stiffness changes of DynaMesh®-IPOM surgical implant due to load history and for different strain ranges is undertaken in this paper. The analysis is based on uni-axial tension failure tests and cyclical loading tests. The experiments respond to load and stretch values that can really act on the implant fixed to the abdominal wall. The research proved that:

- The material stiffness in the initial state and in the preconditioned one differ considerably, in the preconditioned state the mesh is stiffer. The stiffening of the implant increases the reaction forces acting on the joints that fix the mesh. Thus, two states of the mesh should be distinguished in calculations, initial and preconditioned ones. If the preconditioned state of the implant is omitted in calculations considering the number of joints necessary to properly fix the mesh in the abdominal wall, then the number may be underestimated and consequently an increased risk of the fixation damage and recurrence of disease occurs;
- The mesh can be in both of the states (initial and preconditioned) many times, provided that it is not extremely loaded and permanent strains do not occur;
- For the initial state of the material bilinear functions can describe stiffness in the two distinguished directions of the mesh;
- For the preconditioned state of the material nonlinear functions describe its stiffness in the two directions considered. The proposed exponential function well approximates the elastic modulus–strain relation.

Acknowledgements

References

[1] BANSAL V.K., MISRA M.C., KUMAR S., RAO Y.K., SINGHAL P., GOSWAMI A., GULERIA S., ARORA M.K., CHABRA A., *A prospective randomized study comparing suture mesh fixation versus tacker mesh fixation for laparoscopic repair of incisional and ventral hernias*, Surg. Endosc., 2011, 25:1431–1438.

[2] BENSLEY R.P., SCHERMERHORN M.L., HURKS R., SACHS T., BOYD C.A., O'MALLEY A.J., COTTERILL P., LANDON B.E., *Risk of late-onset adhesions and incisional hernia repairs after surgery*, J. Am. Coll. Surg., 2013, 216:1159–1167.

[3] BRANDT S., *Statistical and Computational Methods in Data Analysis* (ed. 3), Springer Verlag, New York, 1997.

[4] DEEKEN C.R., ABDO M.S., FRISELLA M.M., MATTHEWS B.D., *Physicomechanical evaluation of absorbable and nonabsorbable barrier composite meshes for laparoscopic ventral hernia repair*, Surg. Endosc., 2011, 25:1541–52.

[5] ELIASON B.J., FRISELLA M.M., MATTHEWS B.D., DEEKEN C.R., *Effect of repetitive loading on the mechanical properties of synthetic hernia repair materials*. J. Am. Coll. Surg., 2011, 213, 430–435.

[6] HERNÁNDEZ-GASCÓN B., ESPÉS N., PEÑA E., PASCUAL G., BELLÓN J.M., CALVO B., *Computational framework to model and design surgical meshes for hernia repair*, Comput Methods Biomech. Biomed. Eng., 2012, http://dx.doi.org/10.1080/10255842.2012.736967.

[7] HERNÁNDEZ-GASCÓN B., MENA A., PEÑA E., PASCUAL G., BELLÓN J.M., CALVO B., *Understanding the passive mechanical behavior of the human abdominal wall*, Ann. Biomed. Eng., 2013, 41:433–444.

[8] KŁOSOWSKI P., ZAGUBIEŃ A., WOZNICA K., *Investigation on rheological properties of technical fabric Panama*, Arch. Appl. Mech., 2004, 73:661–681.

[9] LI X., KRUGER J., JOR J., NASH M., WONG V., DIETZ P., *Characterizing the ex vivo mechanical properties of synthetic polypropylene surgical mesh*, J. Mech. Behav. Biomed. Mat., 2014, 37:48–55.

[10] LUBOWIECKA I., *Behaviour of orthotropic surgical implant in hernia repair due to the material orientation and abdomen surface deformation*, Comput. Method Biomech., 2013, DOI: 10.1080/10255842.2013.789102.

[11] LYONS R.G., *Understanding Digital Signal Processing*, Addison Wesley Longman Inc., 1997.

[12] MROZOWSKI J., AWREJCEWICZ J., *Foundations of Biomechanics* (in Polish), Łódź, Wydawnictwo Politechniki Łódzkiej, 2004.

[13] PODWOJEWSKI F., OTTÉNIO M., BEILLAS P., GUÉRIN G., TURQUIER F., MITTON D., *Mechanical response of animal abdominal walls in vitro: evaluation of the influence of a hernia defect and a repair with a mesh implanted intraperitoneally*, J. Biomech., 2013, 46, 561–566.

[14] POULOSE B.K., SHELTON J., PHILLIPS S., MOORE D., NEALON W., PENSON D., BECK W., HOLZMAN M.D., *Epidemiology and cost of ventral hernia repair: making the case for hernia research*, Hernia, 2012, 16, 179–183.

[15] RÖHRNBAUER B., OZOG Y., EGGER J., WERBROUCK E., DEPREST J., MAZZA E., *Combined biaxial and uniaxial mechanical characterization of prosthetic meshes in a rabbit model*, J. Biomech., 2013, 46, 1626–1632.

[16] RÖHRNBAUER B., MAZZA E., *Uniaxial and biaxial mechanical characterization of a prosthetic mesh at different length scales*, J. Mech. Behav. Biomed. Mater., 2014, 29, 7–19.

[17] SABERSKI E.R., ORENSTEIN S.B., NOVITSKY Y.W., *Anisotropic evaluation of synthetic surgical meshes*, Hernia, 2011, 15, 47–52.

[18] SONG C., ALIJANI A., FRANK T., HANNA G., CUSCHIERI A., *Elasticity of the living abdominal wall in laparoscopic surgery*, J. Biomech., 2006, 9, 587–591.

[19] STRUSZCZYK M.H., KOMISARCZYK A., KRUCIŃSKA I., GUTOWSKA A., PAŁYS B., CIECHAŃSKA D., *Biomechanical*

Studies of Novel Hernia Meshes with Enhanced Surface Behaviour, FIBRES TEXT, East Eur., 2014, 22, 129–134.

[20] Szepietowska K., Lubowiecka I., *Mechanical behaviour of the implant used in human hernia repair under physiological loads*, Acta Bioeng. Biomech., 2013, 15(3), 89–96.

[21] Szymczak C., Lubowiecka I., Tomaszewska A., Śmietański M., *Investigation of abdomen surface deformation due to life excitation: Implication for implant selection and orientation in laparoscopic ventral hernia repair*, Clin. Biomech., 2012, 27, 105–110.

[22] Szymczak C., Lubowiecka I., Tomaszewska A., Śmietański M., *Modeling of the fascia-mesh system and sensitivity analysis of a junction force after a laparoscopic ventral hernia repair*, J. Theor. Appl. Mech., 2010, 48, 933–950.

[23] Tomaszewska A., Lubowiecka I., Szymczak C., Śmietański M., Meronk B., Kłosowski P., Bury K., *Physical and mathematical modelling of implant-fascia system in order to improve laparoscopic repair of ventral hernia*, Clin. Biomech., 2013, 28, 743–751.

[24] Velayudhan S., Martin D., Cooper-White, J., *Evaluation of dynamic creep properties of surgical mesh prostheses-uniaxial fatigue*, J. Biomed. Mater Res. Part B: Appl. Biomater., 2009, 91, 287–296.